D abstraction by H at a D-saturated Ru(001) surface

T. Yamauchi, Y. Nakashima, T. Misumi, K. Mine, A. Namiki

Department of Electrical Engineering

Kyushu Institute of Technology,

Kitakyushu 804-8550, Japan

(Dated: May 15, 2009)

Abstract

D abstraction (ABS) by H at Ru(001) surfaces initially saturated with D adatoms has been investigated using *in situ* mass spectrometry. HD and D_2 desorption rates are measured at various surface temperatures T as a function of H exposure time. Yield of D_2 desorption increases with T, while that of HD is little affected. Analyzing the measured rate curves, HD and D_2 desorption orders are evaluated to be 1.7 ± 0.1 and 2.5 ± 0.1, respectively, with respect to D coverage θ_D. To pursue the origin of the derived non integral reaction orders the rate curves are further analyzed with the rate equations constructed to involve several ABS channels. Consequently, we find that the HD desorption is mainly governed by a second-order rate law in θ_D rather than the conventional hot atom mediated ABS reaction even when it is corrected to include an isotope effect on ABS. We argue that such second-order ABS kinetics becomes important when the H atoms in excited state of chemisorption have energetically relaxed to some extent, and thereby tend to reside at, e.g. hexagonal closed packed hollow sites, interacting with nearby adatoms. On the other hand, the D_2 rate curves can be fit with third-order kinetics, consistent with the Langmuir-Hinshelwood mechanism in a super-saturation state. The isotope effect plays an essential role in the ABS reaction of D abstraction by H which competes with H abstraction by H as D adatoms are replaced by H atoms.

PACS numbers:

I. INTRODUCTION

The abstraction (ABS) of hydrogen (H) adatoms by gaseous H atoms is of relevance to, e.g., plasma damage of nuclear fusion reactors [1], Si plasma chemical vapor deposition (CVD) for solar cells [2], and the formation of interstellar hydrogen molecules at very cold dust grain surfaces [3]. To date, ABS reactions have been extensively studied with regard to desorption at various metal [4–11], semiconductor [12–19], and graphite [20, 21] surfaces. Isotopic labeling of surface adatoms with D atoms is generally employed to distinguish gas phase H atoms, allowing the elucidation of complex ABS kinetics. Consequently, it has been revealed that both direct ABS (*d*-ABS) and indirect ABS (*id*-ABS) can take place upon exposure of D-covered surfaces to H atoms;

$$(d-\mathrm{ABS}): \quad \mathrm{H}+\mathrm{D/M} \longrightarrow \mathrm{HD}, \tag{1}$$

$$(id-\mathrm{ABS}): \quad \mathrm{H}+\mathrm{D/M} \longrightarrow \mathrm{D_2}. \tag{2}$$

Basic studies of *d*-ABS reactions began with investigation of reaction dynamics, rather than with kinetics, using laser spectroscopy on Cu surfaces [4, 5]. It was found that the translational, rotational and vibrational energies of abstracted molecules were much larger than expected for reactions along a Langmuir-Hinshelwood (LH) mechanism. Because of this energetic desorption, the *d*-ABS reaction was considered as a prototype of an Eley-Rideal (ER) reaction. However, the reaction cross section was evaluated to be approximately 5 Å^2 [6], which is substantially larger than the theoretically evaluated value for the ER reaction ($\leq$0.5 Å^2) [22, 23], suggesting that H atoms react with D adatoms after bouncing a few times over the surface. However, further kinetic studies [7–11] revealed not only the cross-sectional values, but also that the kinetics for both *d*-ABS and *id*-ABS vary depending on the type of metal.

In order to explain the complex kinetics of the ABS reactions, a hot atom (HA) mechanism was invoked [6, 10, 11]. In the HA mechanism, impinging H atoms are first trapped in the excited states of the chemisorption potential, but remain energetically hot by maintaining the chemisorption energy [24]. Therefore, they can hop around the surface and recombine with D adatoms, leading to enlarged ABS reaction cross-sections. Along with the HA scenario, the occurrence of *id*-ABS was interpreted in such terms that the impinging H atoms kick out D adatoms, producing secondary hot D atoms which then abstract other D adatoms.

This is the so-called collision-induced desorption in *id*-ABS.

In such a HA scenario, HD and D_2 desorption induced by H atoms may be expected to obey a first- and a second-order rate law for D coverage θ_D, respectively. That is, the rates of HD and D_2 desorption can be described as $R_{HD} \propto \theta_D$ and $R_{D_2} \propto \theta_D^2$. However, deviation from first-order kinetics has been noted for *d*-ABS reactions, as reported in the literatures [7, 8, 10]. Winkler and his coworkers found that HD desorption on fully saturated surfaces is not purely first-order, but slightly super linear with a non integral reaction order, $R_{HD} \propto \theta_D^{1.3}$ on Ni(110) [7] and $R_{HD} \propto \theta_D^{1.4}$ on Al(100) [8]. Such a deviation from first-order desorption kinetics was also recognized on Pt(111) [10]. Moreover, the initial HD rates at t=0 were found to be independent of D pre-coverages θ_D^0 above 0.4 ML [8]. This unambiguously indicates that hot precursors play a key role in *d*-ABS. Furthermore, a reaction order of 2.5 was determined for the D_2 desorption on Ni(110), i.e., $R_{D_2} \propto \theta_D^{2.5}$ [7], which also deviates from second-order kinetics expected for the HA mechanism. Although the extent of deviation was not determined to be significant for the hot precursor mechanism, Winkler and his collaborators [7, 8] were not insensitive in noticing that the yield of D_2 desorption from unsaturated surfaces was remarkably smaller than expected in the above rate law. For surfaces pre-saturated with, e.g. D adatoms, they are consumed during the ABS reaction, so that the surface saturation must be maintained by quick H adsorption. Therefore, Boh et al. [8] claimed that the impinging H atom, apart from *d*-ABS, can adsorb on such a saturated surface by squeezing into the layer, leading to a local temporary super-saturation state. The surface energy of such a super-saturation state is higher than that at the normal saturation state. The increased surface energy can be lowered by recombinative desorption of adsorbed atoms in a LH reaction, giving rise to *id*-ABS.

Such a super-saturation mechanism, invoked for *id*-ABS on metal surfaces, seems to be indeed in operation on Si surfaces, because *d*-ABS and *id*-ABS were found to obey second- and third- or fourth-order rate laws for θ_D, respectively [14–18]. These unexpectedly high reaction orders implicate that impinging H atoms apparently interact with two D adatoms for *d*-ABS and more than three D atoms for *id*-ABS. Moreover, D_2 desorption from Si(100) and Si(110) surfaces were found to lag as the surface was exposed to a pulsed H beam [25–27]. ¿From a series of investigations [14–19], Namiki and collaborators proposed a hot complex (HC) mechanism [16, 18, 19], by which a H atom is first trapped in the excited state of chemisorption with two adjacent D-Si units. The *d*-ABS reaction can then proceed

during energy relaxation of hot complex. If otherwise the abstraction reaction is detoured the H atom of the hot complex may break the DSi-SiD bond, forming a dihydride. If this occurs on a Si(100)-(3×1) monodeuteride/dideuteride phase, where a unit cell contains four D atoms, the local phase of the D/H/Si system is converted to a (1×1) dihydride phase. Since this phase is thermodynamically unstable [28], the surface energy has to be lowered by emitting a molecule, thereby returning to the original (3×1) phase [25, 26]. If the non-integer reaction order found for *d*-ABS and *id*-ABS on metal surfaces [7, 8, 10] involves such higher order rate terms, it may be worthwhile to reinvestigate the ABS reactions on metal surfaces.

D abstraction by H at Ru surfaces has been less studied [29–31], despite its importance as a catalyst in many hydrogen related reactions. Weinberg and coworkers studied ABS kinetics on a Ru(001) surface [29–31]. Employing temperature programmed-desorption (TPD) spectroscopy, D(H) coverages were measured as a function of H(D) exposure time. In these experiments, *d*-ABS and *id*-ABS were not discriminated, because the desorbed species were not measured. The measured coverage versus fluence curves were fit with a rate equation based on first-order kinetics for *d*-ABS. The cross section of the ABS reaction was evaluated to be less than 1.0 $Å^2$. A strong isotope effect on the ABS reaction was recognized in their experiments, since H abstraction by D occurred much more efficiently than D abstraction by H [31]. However, when applying the first-order kinetics to the measured H(D) coverages versus exposure curves Weiss *et al.* did not take into account the observed isotope effect, which would lead to an apparent deviation from first-order kinetics for the HA-mediated ABS.

In this work, D abstraction by H on the Ru(001) surface is reinvestigated with respect to desorption. To make the ABS reaction system simple we employ mainly saturated surfaces rather than unsaturated surfaces. Thereby complex reaction pathways of sticking to empty sites which may compete with ABS reaction [32] is detoured in elucidating ABS kinetics. Rate curves of HD and D_2 desorptions are analyzed using rate equations constructed similarly to those proposed for Si surfaces [15, 18].

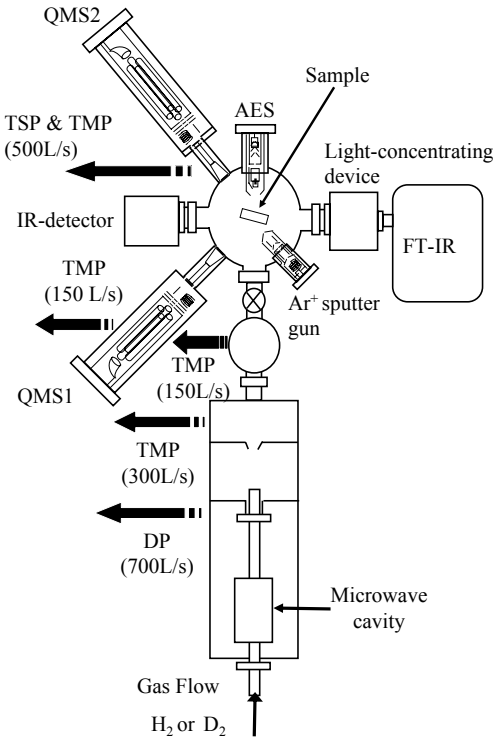

FIG. 1: Experimental set up used for the abstraction reactions on Ru(001). QMS: quadrupole mass spectrometer, TMP: turbo molecular pump, DP: oil diffusion pump, TSP: liquid nitrogen cooled Ti sublimation pump, AES: Auger electron spectrometer.

II. EXPERIMENT

Experiments were carried out in an ultrahigh vacuum chamber (base pressure of 1×10^{-8} Pa) equipped with an Auger electron spectrometer (AES), quadrupole mass spectrometer (QMS), Fourier transform infrared spectroscope (FT-IR), Ar^+ ion sputter gun, atomic beam source and a flow-type liquid He cryostat, which are schematically illustrated in Fig. 1. A Ru(001) single crystal (diameter: 10 mm, thickness: 2 mm) was spot welded to a tantalum plate, which was attached to a copper holder via a sapphire plate for electrical insulation, but thermal conduction. A K-type thermocouple was spot welded to the side of the sample disc, enabling monitoring of the sample temperature, T. The Ru(001) surface was cleaned by cycles of 1 keV Ar^+ ion sputtering at 300 K, combined with surface oxidation using O_2 gas, followed by combustion of carbon contaminants at 1500 K. The AES spectrum showed

that impurities such as O and C were not present on the surface. The H(D) beam generator consists of three differentially pumped chambers to assure a base pressure as low as 1×10^{-7} Pa in the reaction chamber, even under beam operation. The first chamber is equipped with a cylindrical plasma cavity, to which a 4.23 GHz microwave power of 300 W was applied to generate D and H atoms from D_2 and H_2 gases. The mean kinetic energy of H atoms is 47±3 meV which was determined from the time-of-flight distribution measured with a cross-correlation random chopper [33]. In order to enhance the H flux, H_2 gas was mixed with a small amount of O_2 gas (2% of H_2 pressure). A H flux of $2\pm1 \times 10^{12}\mathrm{s}^{-1}\mathrm{cm}^{-2}$ was evaluated by directly measuring the dissociated H_2 gas with a QMS. Although the amount of oxygen adsorbed during H exposure was not measured, due to the relatively small flux of O_2 and H_2O converted in the plasma, taking the consumption of D adatoms in the early stages of H exposure and the possible elimination of O adatoms by H atoms [34] into consideration, the effect of possibly adsorbed oxygen atoms on the ABS kinetics was expected to be small. D and H irradiation was started and stopped by manually controlling a gate valve between the reaction chamber and the third chamber. In order to flush out residual D species in the beam system, the entire beam system was evacuated, and then further flashed out with H_2 plasma for 4-5 min before opening the gate valve. This was also necessary to obtain a stable H flux. Desorbed HD and D_2 molecules were detected using two QMSs. One QMS was set at a position far below the sample to detect desorbed molecules in an angle integrated mode. The other QMS was located in a differentially pumped chamber to directly detect desorbed molecules. The angle between the beam and the QMS axis was fixed at 30°. A third QMS was set to monitor the H(D) beams. In this work, the first QMS was mainly used to measure molecular desorption in an angle integrated mode.

To analyze HD and D_2 rate equations, rate versus t curves were converted to rate versus θ_D curves, by evaluation of θ_D from

$$\theta_\mathrm{D}(t) = \int_t^{t_m} [R_\mathrm{HD}(t) + 2R_{\mathrm{D}_2}(t)]dt + \theta_\mathrm{D}(t_m), \tag{3}$$

where t_m is the time when H exposure was stopped, and $R_\mathrm{HD}(t)$ and $R_{\mathrm{D}_2}(t)$ are the rates of HD and D_2 molecules at t, respectively [14]. The coverage at t_m was evaluated from HD and D_2 TPD spectra when H exposure was stopped. The saturated D coverage was calibrated to be 1.0 ML after referring to the report by Weiss et al. [31].

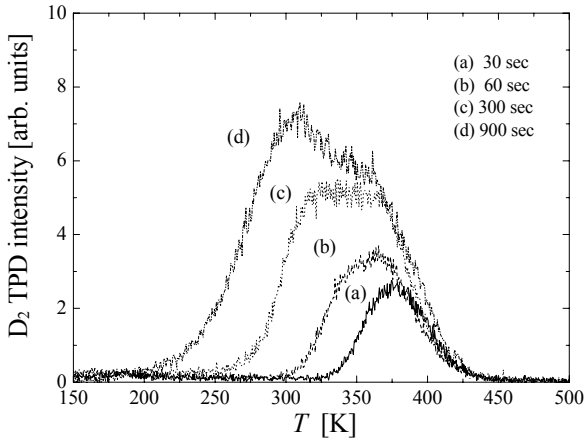

FIG. 2: Plots of D_2 TPD spectra measured for various D dosing time. Heating rate is 0.5 K/s.

III. RESULTS AND DISCUSSION

A. Hydrogen adsorption sites

The clean Ru(001) surface was exposed to D atoms for preparation of the D-covered surface. Figure 2 shows plots of D_2 TPD spectra obtained for various D dosing at 80 K. With increasing D dose, the D_2 TPD peak increased in intensity and shifted to lower temperatures. This feature is in good agreement with the dissociative adsorption of molecules [35, 36]. The TPD spectra obtained for D dosing shorter than 100 s appear to consist of a single component. On the other hand, the spectra tend to exhibit a second component with further increase in D dosing time up to 900 s, with an apparent peak at around 300 K and a shoulder at around 370 K. The peak intensity nearly leveled off at 900 s, suggesting that the surface was mostly saturated at this dose. According to Weiss *et al.* [31], D adsorption onto a Ru(001) surface saturates at 1 ML (ML: mono layer of one D atom per surface Ru atom) when D atoms are generated by means of a microwave plasma; the same method employed in the present work. Recent scanning tunneling microscopy (STM) studies [37] have revealed that hydrogen atoms adsorb at fcc (face centered cubic) hollow sites. Therefore, it should be noted that in the present study, H atoms abstract D adatoms that are adsorbed at fcc hollow sites. Figure 3 illustrates the model of structure of a Ru(001) surface saturated with $\sim$ 1.0 ML D(H) adatoms.

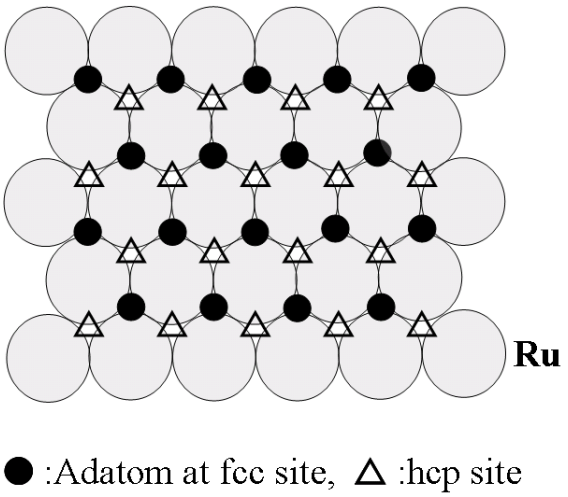

FIG. 3: Atomic arrangement of saturated adatoms on the Ru(001) surface. At saturation with 1.0 ML adatoms, all the fcc hollow sites are occupied by adatoms. Open triangles depict the hexagonal closed packed (hcp) hollow sites.

B. HD and D_2 Rate curves

The D-saturated surface was exposed to H atoms at various surface temperatures. Multiplex operation of the QMS allowed the simultaneous measurement of H_2, HD and D_2 desorption. High desorption rates were observed for HD and D_2 molecules, although the QMS signals of desorbed H_2 molecules were almost obscured by the strong H_2 background. Therefore, only the HD and D_2 rate curves were analyzed. Representative rate curves measured at 111, 150 and 196 K are plotted as a function of H exposure time t in Fig. 4. Both the HD and D_2 rates jump up at t=0; the HD rate curves immediately attain the peak maximum at $t \simeq 0$, while the peak maximum of the D_2 rate lags. The apparent peak maximum appears at 9, 11.4, and 13.8 s at 111, 150, and 196 K, respectively. The delay of the peak is more pronounced at 196 K than at 111 K. After the peak maximum, the HD and D_2 rates both decrease quite sharply, due to loss of the surface D adatoms by the ABS reaction. However, it should be noted that loss of D atoms by ABS are compensated by quick adsorption of H atoms during H exposure, thereby maintaining surface saturation [29, 31]. The decrease of the rate curves is much faster for D_2 than for HD molecules.

HD and D_2 rate curves were also measured for the 0.6 ML D-covered Ru(001) surfaces that were prepared by 250 K annealing of the presaturated surface. We found that the

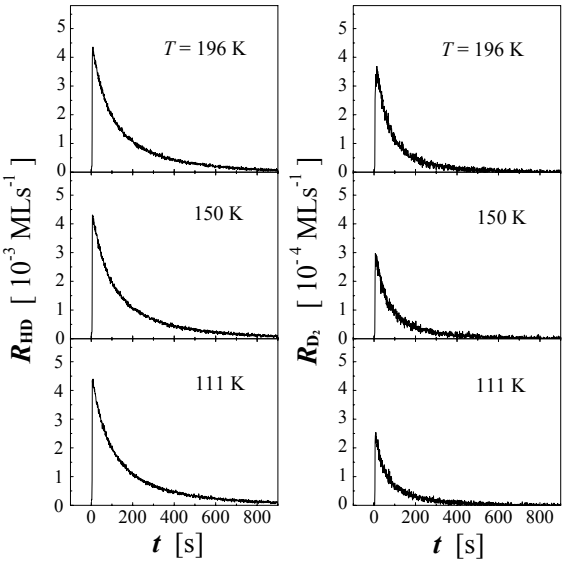

FIG. 4: Plots of HD (left panel) and D_2 (right panel) desorption rates as a function of H exposure time t at T=111, 150 and 196 K. The apparent peak maximum in the D_2 desorption rate curves appears at 9, 11.4, and 13.8 s at 111, 150, and 196 K, respectively.

maximum rate of the HD desorption at t=0 was almost the same to those on the saturated surface. Similar result was also recognized on the Al surface by Boh *et al.* [8] who considered that it is the evidence of the hot precursor-mediated mechanism. On the other hand, the rate of D_2 desorption was considerably smaller than that on the saturated surface. Taking the case at T =150 K, for example, the maximum D_2 desorption rate was nearly one tenth of the rates measured on the saturated surface. Because of the poor signal to noise ratio, the measured D_2 rate curves were not able to be analyzed for this study.

If the LH mechanism governs the ABS reaction, then HD and D_2 desorption would be temperature dependent. However, the HD rates plotted in Fig. 4 exhibit almost no significant influence of temperature, whereas the measured D_2 rate curves do show a certain trend of increasing rate with T. This feature can be clearly seen in Fig. 5, where fractions of the abstracted HD and D_2 yield are plotted as a function of T. The D_2 yield increases with T, suggesting that the *id*-ABS process is of LH type. In contrast, the total HD yield is almost constant. The lack of significant dependence of desorption on T indicates that the nature of the HD desorption is mostly direct.

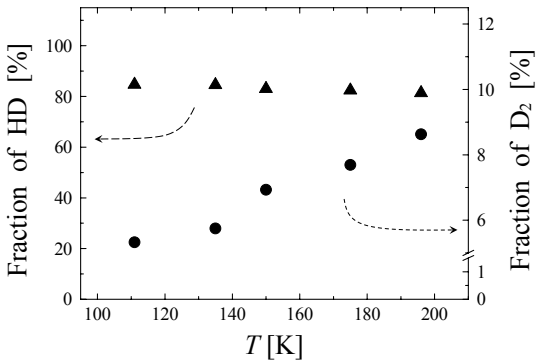

FIG. 5: Plots of fractions of desorbed HD and D_2 yield as a function of T. In these experiments nearly 0.9 ML D adatoms were removed by H atoms.

C. Rate equation analysis

In order to understand the kinetic mechanisms of the *d*- and *id*-ABS reactions, rates versus t curves should be converted to rates versus $\theta_{\rm D}$ curves. Momentary surface D coverages $\theta_{\rm D}$ during ABS reactions were evaluated using Eq. 3 as a function of t for various temperatures. Figure 6 shows plot of the $\theta_{\rm D}$ versus t curve obtained for $T = 111$ K. Then, the rate curves plotted as a function of t in Fig. 4 were converted to rate versus $\theta_{\rm D}$ curves. Results were plotted in Fig. 7.

To estimate ABS reaction order from a surface coverage perspective, first we fit the $\theta_{\rm D}$ vs. t curve plotted in Fig. 6 with a first-order, $\theta_{\rm D} = \exp(-kt)$, and second-order, $\theta_{\rm D} = 1/(1+kt)$, kinetics curve. Here these two kinetics curves were obtained under the condition that $\theta_{\rm D}(0) = 1$ ML. From comparison of the two fit curves plotted in Fig. 6, one can easily find that the second-order fit ($k = (719 \pm 3) \times 10^{-5}{\rm ML}^{-1}{\rm s}^{-1}$) is much better than the first-order fit ($k = (346 \pm 2) \times 10^{-5}{\rm s}^{-1}$), suggesting that the ABS reaction apparently follows a second-order kinetics. If the HD desorption via *id*-ABS paths may be small as suggested by the D_2 yield plotted in Fig. 5, the *d*-ABS reaction may be expected to follow second-order kinetics rather than first-order kinetics [31]. However, one may notice that there is a systematic, small deviation from the true second-order kinetics and therefore we

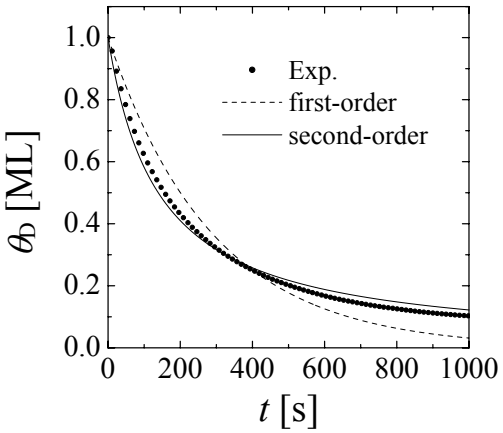

FIG. 6: Plots of $\theta_{\rm D}$ as a function of t, and fits with the first-order (dashed line: $\theta_{\rm D} = \exp(-kt)$ with $k = 3.46 \times 10^{-3}$ s^{-1}) and second-order (solid line: $\theta_{\rm D} = 1/(1+kt)$ with $k = 7.19 \times 10^{-3}$ ML^{-1} s^{-1}) rate curves. The experimental curve was obtained using eq.(3) in the text for the HD and D_2 rate curves measured at 111 K.

need to know more realistic desorption order using a general rate equation. This may be actually done by fitting the HD and D_2 rates versus $\theta_{\rm D}$ curves with a general rate equation, $R_i \propto \theta_{\rm D}^m$, where R_i is the rate of desorption of i(=HD or D_2) molecules, and m is the reaction order. A portion of the rate curves after the apparent peak maximum was fit, and as a result, $m = 1.7 \pm 0.1, 1.65 \pm 0.10$, and 1.6±0.1 were obtained for HD desorption at T=196, 150, and 111 K, respectively, while $m = 2.5 \pm 0.1, 2.4 \pm 0.1$, and 2.5±0.10 were obtained for D_2 desorption at T =196, 150, and 111 K, respectively. Thus, it is quite obvious that the reaction orders for both HD and D_2 desorptions are larger than that anticipated in the HA mechanism.

The manner of D abstraction by H on the Ru(001) surface appears to be quite similar to that on Ni [7] and Al [8] surfaces. As stated in the Introduction, Winkler and his colleagues [7–9] invoked the hot precursor-mediated-mechanism for *d*-ABS and the collision-induced LH mechanism for *id*-ABS, which occurs via temporary super-saturation of adatoms. Moreover, possible kinetic mechanisms implicated in the observed deviation from the HA mechanism which obeys a second-order kinetics must be analogous to those on Si(111) [18].

The value of $m \simeq$1.6-1.7 obtained for HD desorption suggests that a possible equation for the *d*-ABS may include a term characterized with second-order kinetics in $\theta_{\rm D}$. Furthermore, the value of $m \simeq 2.5$ obtained for the D_2 *id*-ABS suggests that a possible rate equation for

the *id*-ABS may include third-order rate terms in $\theta_{\rm D}$ and $\theta_{\rm H}$. Therefore, rate equations for the ABS reaction at the Ru(001) surface can be constructed similarly to the rate equations constructed for the ABS reactions at Si(111) surfaces [18]. Namely, depending on the extent of energy relaxation of H atoms in chemisorption potentials at the surface we claim three distinctive ABS channels referred to as HA, HC, and LH channel. Desorptions along the HA and HC channels are hot atom and hot complex mediated reactions, respectively, both being categorized to *d*-ABS. The LH channel is related to the temperature dependent LH reactions, being categorized to *id*-ABS.

The D_2 desorption along the third-order LH channel may occur at sites which are locally saturated with three D adatoms (3D configuration) or two D and one H adatoms (2D1H configuration). Transient adsorption of a H atom at, e.g. hexagonal closed packed (hcp) hollow sites (see Fig. (3)) results in a local super saturation state. In order to reduce the excess surface energy, so formed super-saturation state will expel a molecule. In this case the excess H atom is not involved in the molecule. D_2 molecules will be exclusively emitted from sites with 3D configuration. On the other hand, at sites with 2D1H configuration, either D_2 or HD desorption can take place competitively, probably receiving an isotope effect [18].

The D_2 rate curves plotted in Fig. 4 or in Fig. 7 have a time lag in getting to the maximum rate, suggesting that achieving such a super-saturation state takes induction time even at the 1 ML coverage. This was also observed on Si(111) where an *S*-shaped sigmoid curve, referred to as $\eta(t)$, was employed to describe its time profile [18]. For the ABS reactions at the Ru(001) surface we use the same η,

$$\eta(t) = \frac{1}{2}[1 + {\rm erf}(\frac{\theta_{\rm D+H}(t) - \vartheta_{\rm D}^0}{\omega(T)})], \tag{4}$$

where erf is the error function, and $\vartheta_{\rm D}^0$ and ω are the coverages to give the steepest slope and width of the curve, respectively. The value of 1.0 ML was chosen for $\vartheta_{\rm D}^0$ for all temperatures, while the values of ω (=1.1, 1.66, and 3.28×10^{-3} ML for T=111, 150, and 196 K, respectively) were chosen so that the rising and peaking of each D_2 rate curve plotted in Fig. 7 could be reproduced. As directly observed [38] and simulated [39] on Si(100) surface, the steady state coverage during H exposure must be larger than the saturated coverage measured after ceasing exposing to H atoms. Considering this possible oversaturation during H exposure, it was assumed that $\theta_{\rm H+D}$ increases with t according to the equation $\theta_{\rm D+H}(t)(=\theta_{\rm H}+\theta_{\rm D}) = 1.0 + 3.67\times10^{-4}\,t$. This increase of the total coverage caused η to gradually increase to

unity, after which $\theta_{\mathrm{H+D}}$ was set to 1.02 ML referencing the value obtained by sufficient D fluence [31]. The η used for the curve fits were plotted in Fig. 8. One should note that only the late half of a sigmoid curve for $\eta > 0.5$ is used and hence it does not look like S.

Taking the above mentioned consideration into account, we invoke the following rate equation for the D_2 desorption,

$$R_{\mathrm{D}_2} = b\,\theta_{\mathrm{D}}^2 + \eta(t)[k_1\theta_{\mathrm{D}}^3 + k_2\theta_{\mathrm{D}}^2\theta_{\mathrm{H}}], \tag{5}$$

where the second-odrer rate term with the rate constant b describes the HA mediated collision-induced-desorption paths, while the third-order rate terms describe the LH type *id*-ABS paths. k_1 and k_2 are the rate constants for the *id*-ABS reactions at sites with 3D and 2D1H configuration, respectively. As a result of least mean squares curve fit analysis, we found that the first term $b\,\theta_{\mathrm{D}}^2$ should be omitted since the best fits were obtained as it became zero or negative. This fact seems to be sound reasonable since the collision-induced-desorption process is a generalized ER reaction and hence it must receive little temperature effect [24]. However, this is not the present case as shown in Fig. 5.

On the other hand, the HD rate equation consists of three rate terms of the HA, HC, and LH channel. In contrast to Si surfaces where H chemisorption potential is so highly corrugated that hot atoms cannot migrate over the surface [16], hot atoms on the Ru(001) surface may migrate across the surface overcoming less corrugated potential barriers. Therefore, hot H atoms interact with D adatoms as well as H adatoms accumulated during H exposure. Because of the isotope effect, the probability of D abstraction by H, p_{D}, must be smaller than the probability of H abstraction by H, p_{H}. This isotope effect on the HA channel should be taken into consideration for the actual ABS reactions. The HA-mediated, Kisliuk type ABS rate equation was formulated as follows. Suppose that the Ru(001) surface is saturated with coadsorbed H and D adatoms at the mid stages of the surface exposure to H atoms. A hot atom makes binary collision with an adatom to generate *d*-ABS. If otherwise it fails the ABS reaction, the hot atom will migrate to the neighboring site to try the ABS reaction again. The migration probability can be written as $p_m = 1 - p_{\mathrm{D}}\theta_{\mathrm{D}} - p_{\mathrm{H}}\theta_{\mathrm{H}}$. Here the terms $p_{\mathrm{D}}\theta_{\mathrm{D}}$ or $p_{\mathrm{H}}\theta_{\mathrm{H}}$ stands for the adatom abstraction probability when the site visited by the H atom is occupied by a D or H adatom. On the saturated surfaces, total coverage during H exposure is assumed to keep 1 ML, i.e., $\theta_H + \theta_D = 1$. The probability to generate HD *d*-ABS

through the HA channel can be expressed as,

$$P_{\rm HD} = p_{\rm D}\theta_{\rm D} + p_m p_{\rm D}\theta_{\rm D} + p_m^2 p_{\rm D}\theta_{\rm D} + \cdots\cdots, \tag{6}$$

$$= (1 + \frac{p_{\rm H}}{p_{\rm D}}(\frac{1}{\theta_{\rm D}} - 1))^{-1}. \tag{7}$$

One should note that if no isotope effects are present, i.e., $p_{\rm H} = p_{\rm D}$, a first-order kinetics, $P_{\rm HD} = \theta_{\rm D}$, can be derived. On the contrary, if $p_{\rm H} > p_{\rm D}$, the HD rate curves deviate from the first-order kinetics as will be shown later.

Consequently, the proposed HD rate equation can be written as,

$$R_{\rm HD} = c_1(1 + \frac{p_{\rm H}}{p_{\rm D}}(\frac{1}{\theta_{\rm D}} - 1))^{-1} + c_2\,\theta_{\rm D}^2 + c_3\,\eta(t)\theta_{\rm D}^2\theta_{\rm H}. \tag{8}$$

Here, the first, second, and third terms in the right hand side stem from the HA, HC, and LH channel desorptions, respectively. In eq. (8), we have omitted to write other possible terms proportional to $\theta_{\rm D}\theta_{\rm H}$ and $\eta(t)\theta_{\rm D}\theta_{\rm H}^2$ since they turn out to be less important in the curve fittings due to isotope effects.

The experimental rate curves plotted in Fig.7 were fit with the above rate equations (5) and (8) for the D_2 and HD ABS reactions, respectively. Results of the best fits of HD and D_2 rate curves were plotted in the left and right panel of Fig. 7. The values of parameters to give the best fits were summarized in the caption of Fig. 7. Notice that D_2 desorption along the *id*-ABS paths is mostly governed by the desorption from the 3D configuration. The negligible D_2 desorption from the 2D1H configuration is due to isotope effect ($c_3/k_2 \simeq 20$) which makes HD desorption easier than D_2 desorption from the same configuration.

The decomposed HD rate curves plotted in Fig. 7 show up that the HC-mediated channel is the major path among the three ABS channels. Take the data for $T = 196$ K, for example, the yield ratio of each ABS component to the total one is 0.24, 0.52, and 0.24 for the HA, HC, and LH channel, respectively. The predominance of the ABS reaction along the HC channel suggests that the majority of the ABS reaction proceeds via simultaneous interaction of H atoms with two D adatoms.

However, the rate curves related to the HA-mediated component exhibits a considerable deviation from first-order kinetics due to the isotope effect $p_{\rm H}/p_{\rm D} > 1$, and hence the curves of the HA-mediated path look like nearly second-order kinetics. This might lead us to such an idea that the experimental rate curves could be fit even without the contribution from the HC channel. Therefore, we tested two cases, (a) : $R_{\rm HD} = c_1(1 + \frac{p_{\rm H}}{p_{\rm D}}(\frac{1}{\theta_{\rm D}} - 1))^{-1}$, and

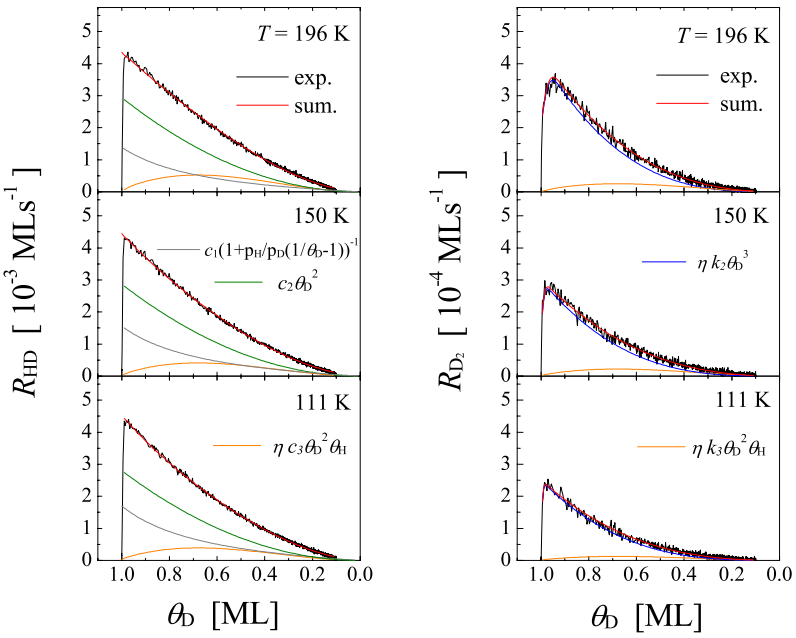

FIG. 7: Plots of HD and D_2 rate curves and their fits with rate equations Eqs. 5 and 8 in the text. The fit parameters for D_2 rate curves $(k_1(10^{-3}/\mathrm{ML\ s}), k_2(10^{-3}/\mathrm{ML}^2\ \mathrm{s})$ are (0.25, 0.08), (0.30, 0.14), and (0.42, 0.16) at 111, 150, and 196 K, respectively. For the HD desorption rate curves, the fit parameters $(c_1(10^{-3}/\mathrm{s}), c_2(10^{-3}/\mathrm{ML\ s}), c_3(10^{-3}/\mathrm{ML}^2\ \mathrm{s}))$ are (1.70, 1.58, 1.29), (2.80, 2.87, 2.94), (2.48, 2.61, 3.33), and $p_\mathrm{H}/p_\mathrm{D} = 3.55 \pm 0.22, 3.56 \pm 0.30$, and 3.61 ± 0.35 at 111, 150, and 196 K, respectively. The standard deviations of k_i for $i = 1, 2$ and c_j for $j = 1, 2, 3$ are at most 1% of the value of each rate constant.

$(b) : R_\mathrm{HD} = c_1(1 + \frac{p_\mathrm{H}}{p_\mathrm{D}}(\frac{1}{\theta_\mathrm{D}} - 1))^{-1} + c_3\eta(t)\theta_\mathrm{D}^2\theta_\mathrm{H}$. As a result of the best curve fits, we found that both (a) and (b) rate equations had a systematic deviation from the experimental rate curves, leading to poorer fits than the above fits that included the HC-mediated rate term.

We now give some speculative explanation about the possible origins of the HA, HC, and LH channel. At the early stages of their chemisorption to the locally saturated sites, H atoms are still energetically high keeping the adsorption energy, and thus they can visit D or H adatoms many times migrating from site to site at the surface. The HA channel could be related to this process. However, meanwhile the hot atoms lose their excess energy and then they tend to reside for a while at energetically metastable sites where they can interact with two D adatoms to abstract one of them. The HC channel could be categorized to this

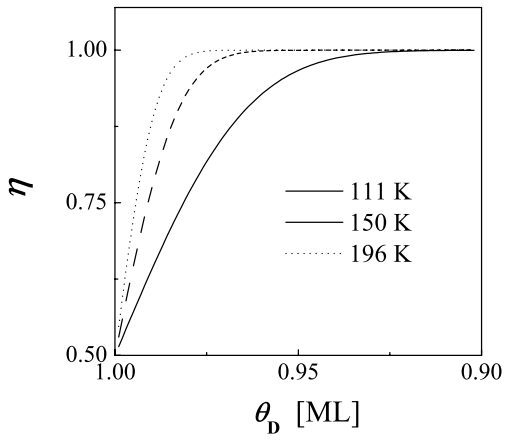

FIG. 8: Plots of the calculated η function for T=111, 150, and 196 K.

process. If both of the HA and HC channels are detoured, the H atoms will be energetically relaxed further, rendering themselves in the local super-saturation state at, *e.g.* hcp hollow sites marked in Fig. 3. Such a local super-saturation state must be thermodynamically unstable because of the excess H atoms. Thereby a molecule would be finally emitted from the super-saturation states. The HD as well as D_2 desorptions along the LH channel could be ascribed to this process. In this idea we think of that relative contribution of the HC channel to the HA channel strongly depends on the rate of energy relaxation of chemisorbed H atoms. Electron-hole pair creation by H adsorption [40, 41] may be one of the possible energy loss channel and therefore yield ratios of the HC to the HA channel will vary from metal to metal.

Finally, we give some discussion on the isotope effect on ABS. On the basis of the above mentioned Kisliuk type rate equation analysis, we found considerable isotope effect on the HA channel. Namely, the H abstraction by H is nearly 3.5 times efficient than D abstraction by H. Similar isotope effect on the ABS reactions was reported on Ru(001) by Weiss et al. [31] who found that the H abstraction by D is nearly two times more efficient than the D abstraction by H.

At Si(100) surfaces strong isotope effect on ABS was also directly measured in the preferred D adsorption to the H adsorption as the surfaces were exposed to mixed H and D atoms with the same flux [42, 43]. In this case, D and H uptake curves can be reproduced in a Monte Carlo simulation based on the strong isotope effect on ABS [43]. Since the *d*-ABS

at the Si surfaces proceeds solely along the HC channel, the strong isotope effect claims selective H abstraction by H at sites with 1D1H configuration. Similar isotope effect on ABS may be expected even at the Ru(001) surface when excess H atoms visit sites with 1D1H configuration. This is the reason why another second-order rate term proportional to $\theta_D\theta_H$ has been omitted from Eq. (8).

Such isotope effect can be also noticed even in the HD and D_2 desorptions through the LH channel occurring at the same 2D1H configuration. As analyzed in Fig. 7, we find that the rate constant c_3 is larger than k_2 by a factor of about 20. Generally speaking, lighter H adatoms can be easily abstracted than heavier D adatoms because of possible quantum effects on reaction rate constants reflecting zero point vibrational energy-affected barriers, attempting frequency factors, tunneling probabilities through reaction barriers, etc. For reaction systems such as H-induced ABS reactions at H and D coadsorbed surfaces, isotope effects cannot be ignored in analyzing measured ABS rate curves.

IV. SUMMARY

D abstraction by H at D/Ru(001) surfaces was investigated with respect to desorption using *in situ* mass spectrometry. HD and D_2 molecules were found to desorb from the *D*-covered Ru(001) surface under exposure to H atoms. The desorption of HD molecules was less T sensitive, whereas the D_2 desorption yield increased with T. The kinetic orders of the abstraction reaction with respect to θ_D were determined to be 1.7±0.1 and 2.5±0.1 for HD and D_2 molecules, respectively. These values are apparently larger than the values expected for the hot atom-mediated *d*-ABS (first-order) and *id*-ABS (second-order) reactions. Rate equations for HD and D_2 desorption were constructed similarly to the case at the Si(111) surface. The D_2 rate equation was constructed on the basis of third-order kinetics for θ_H and θ_D, referred to as Langmuir-Hinshelwood (LH) channel. The proposed HD rate equation consisted of hot atom (HA)-mediated (deviated first-order kinetics due to isotope effect on ABS), hot complex (HC) mediated (second-order kinetics), and a LH channel (third-order kinetics). The HA-mediated ABS rate was obtained by a Kisliuk model after including isotope effect on ABS probability. The measured HD and D_2 rate curves were then fit with

the their rate equations to determine the contribution of each rate term. As a result, the HC-mediated ABS was found to be predominant over the HA-mediated ABS. The *d*-ABS reaction could be interpreted in terms of simultaneous interaction of a H atom with two D adatoms. Isotope effect on the *d*- and *id*-ABS reactions was found to be crucial as the surfaces were coadsorbed by H and D atoms during the exposure to H atoms.

Acknowledgments

The authors express their sincere thanks to A. Winkler for discussion on the HA-mediated ABS. They also thank to J. Yoshinobu for his advice in constructing the experimental set up. This work was financially supported by a Grant-in-Aid for Specially-promoted Research (No. 17002011) and Young Scientists (B) (No. 20740140) of the Ministry of Education, Culture, Sports, Science, and Technology of Japan.

---

[1] A. W. Kleyn, W. Koppers and N. L. Cardozo, Vacuum **80**(2006)1098.

[2] M. Kondo and A. Matsuda, Thin Solid Films **383**(2001)1.

[3] J. M. Greenberg, Surf. Sci. **500**(2002)793.

[4] C. T. Rettner, Phys. Rev. Lett. **69**(1992)383.

[5] C. T. Rettner and D. J. Auerbach, Phys. Rev. Lett. **74**(1995)4551.

[6] C. T. Rettner and D. J. Auerbach, J. Chem. Phys. **104**(1996)2732.

[7] G. Eilmsteiner, W. Walkner, and A. Winkler, Surf. Sci. **352-354**(1996)263.

[8] J. Boh, G. Eilmsteiner, K. D. Rendulic, and A. Winkler, Surf. Sci. **395**(1998)98.

[9] H. Pölzl, G. Strohmeier, and A. Winkler, J. Chem. Phys. **110**(1999)1154.

[10] S. Wehner and J. Küppers, J. Chem. Phys. **108**(1998)3353.

[11] J. -Y. Kim and J. Lee, (a): Phys. Rev. Lett. **82**(1999)1325, (b): J. Chem. Phys. **113**(2000)2856.

[12] S. A. Buntin, J. Chem. Phys. **108**(1998)1601.

[13] A. Dinger, C. Lutterloh, and J. Küppers, Chem. Phys. Lett. **311**(1999)202.

[14] S. Shimokawa, A. Namiki, T. Ando, Y. Sato, and J. Lee, J. Chem. Phys. **112**(2000)356.

[15] F. Khanom, S. Shimokawa, S. Inanaga, A. Namiki, M. N. Gamo, and T. Ando, J. Chem. Phys. **113**(2000)3792.

[16] E. Hayakawa, F. Khanom, T. Yoshifuku, S. Shimokawa, A. Namiki, and T. Ando, Phys. Rev. **B 65**(2001)033405.

[17] A. Kubo, Y. Ishii, and M. Kitajima, J. Chem. Phys. **117**(2002)11336.

[18] F. Khanom, A. Aoki, F. Rahman, and A. Namiki, Surf. Sci. **536**(2003)191.

[19] A. R. Khan, Y. Narita, A. Namiki, A. Kato, and M. Suemitsu, Surf. Sci. **602**(2008)1979.

[20] S. C. Creighan, J. S. A. Perry, and S. D. Price, J. Chem. Phys. **124**(2006)114701.

[21] F. Islam, E. R. Ratimer, and S. D. Price, J. Chem. Phys. **127**(2007)064701.

[22] S. Caratzoulas, B. Jackson, and M. Persson, J. Chem. Phys. **107**(1997)6420.

[23] B. Jackson and D. Lemoine, J. Chem. Phys. **114**(2001)474.

[24] J. Harris and B. Kasemo, Surf. Sci. **105**(1981)L281.

[25] F. Rahman, M. Kuroda, T. Kiyonaga, F. Khanom, H. Tsurumaki, S. Inanaga, and A. Namiki, J. Chem. Phys. **121**(2004)3221.

[26] S. Inanaga, H. Goto, A. Takeo, F. Rahman, F. Khanom, and A. Namiki, Surf. Sci. **596**(2005)82.

[27] A. R. Khan, A. Takeo, S. Ueno, S. Inanaga, T. Yamauchi, Y. Narita, H. Tsurumaki, and A. Namiki, Surf. Sci. **60**(2007)11635.

[28] J. E. Northrup, Phys. Rev. **B 44**(1991)1419.

[29] T. A. Jachimowski and W. H. Weinberg, J. Chem. Phys. **101**(1994)10997.

[30] T. A. Jachimowski, B. Meng, D. F. Jhonson, and W. H. Weinberg, J. Vac. Sci. Technol. **A 13**(1995)1564.

[31] M. J. Weiss, C. J. Hagedorn, and W. H. Weinberg, Surf. Sci. **429**(1999)54.

[32] T. Kammler, D. Kolovos-Vellianitis, and J. Küppers, Surf. Sci. **460**(2000)91.

[33] D. Ogasawara and A. Namiki, unpublished results.

[34] Y. Iwasaki, A. Izumi, H. Tsurumaki, A. Namiki, H. Oizumi and I. Nishiyama, Appl. Surf. Sci. **253**(2007)8699.

[35] P. Feulner and D. Menzel, Surf.Sci. **154**(1985)465.

[36] K. L. Kostov, W. Widdra, and D. Menzel, Surf. Sci. **560**(2004)130.

[37] M. Tatarkhanov, F. Rose, E. Fomin, D. F. Ogletree and M. Salmeron, Surf. Sci. **602**(2008)487.

[38] A. Kutana, B. Makarenko, and J. W. Rabalas, J. Chem. Phys. **119**(2003)11906.

[39] S. Inanaga, F. Rahman, F. Khanom, and A. Namiki, J. Vac. Sci. Technol. **A 23**(2005)1471.

[40] B. Gergen, H. Nienhaus, W. H. Weinber, E. W. McFarland, Science 294(2001)2521.

[41] H. Nienhaus, B. Gergen, W. H. Weinberg, E. W. MacFarland, Surf. Sci. 514(2002)172.

[42] M. C. Hersam, N. P. Guisinger, J. Lee, K. Cheng, and J. W. Lyding, Appl. Phys. Lett. **80**(2002)201.

[43] F. Rahman, N. Onishi, F. Khanom, S. Inanaga, and A. Namiki, Jpn. J. Appl. Phys. **43**(2004)726(2004).